Investigation of quasi-one-dimensional finite phononic crystal with conical section

ZHIQIANG FU[1,2,*], SHUYU LIN[2], SHI CHEN[2], XIAOJUN XIAN[2,3] and CHENGHUI WANG[1]

[1]School of Science, Xi'an University of Architecture and Technology, No. 13, Yanta Road, Xi'an, Shaanxi 710055, People's Republic of China
[2]Institute of Applied Acoustics, Shaanxi Normal University, No. 199, Chang'an South Road, Xi'an, Shaanxi 710062, People's Republic of China
[3]China Electronics Technology Group Corporation 26th Research Institute, Chongqing 400060, People's Republic of China
*Corresponding author. E-mail: fuzhi2004@sohu.com (Z Q Fu), sylin@snnu.edu.cn (S Y Lin)

Abstract. In this paper, we studied the propagation of elastic longitudinal waves in quasi-one-dimensional (1D) finite phononic crystal with conical section, and derived expressions of frequency-response functions. It is found that, contrary to the 1D phononic crystal with a constant section, the value of attenuation inside the band gaps decreases quickly when cross-sectional area increases, and the initial frequency also decreases, but the cut-off frequency increases, thus the width of the band gap increases. The effects of lattice constant and the filling fraction on the band gap are also analysed, and the change trends of the initial frequency and cut-off frequency are consistent with those of constant section. It is shown that the results using this method are in good agreement with the results analysed by the finite element software, ANSYS. We hope that the results will be helpful in practical applications of phononic crystals.

Keywords. Finite phononic crystal; band gap; frequency-response functions.

PACS Nos   **43.20.+g; 43.40.+s; 63.20.−e**

1. Introduction

In recent years, the propagation of classical waves in disordered systems in many fields, such as electron waves in solids, optical waves in dielectric mediums and acoustic waves in elastic mediums, has been studied widely. The propagation of optical waves in periodic dielectric composite materials, known as photonic crystals, was first presented by Yablonovitch [1] and John [2]. By analogy with the photonic crystals, the propagation of elastic/acoustic waves in periodic structures made of materials with different elastic

properties has received a great deal of attention. The artificially made periodic elastic/acoustic structures are called phononic crystals (PCs), and the PCs exhibit phononic band gap (PBG) as the photonic crystal, i.e. the sound and vibrations in the band gap are forbidden [3–24]. There are two common methods to generate PBG, namely, Bragg scattering and local resonances. For Bragg scattering, the first-frequency band gap is the order of wave speed of the medium divided by the lattice constant. So, in order to obtain a low-frequency band gap, it is necessary to use high density/low modulus materials or large size structures [4,5]. For local resonances, band gaps can be obtained at much lower frequencies than those by Bragg scattering. However, heavy resonators are needed to obtain wide band gaps [6].

Several computational methods, such as transfer-matrix (TM) method [10–12], plane-wave expansion (PWE) method [13,14], finite difference time domain (FDTD) method [15,16], multiple scattering theory (MST) [17,18] and finite element (FEM) method [19], have been used to predict the elastic/acoustic band structures. Discrete models are also used to calculate the band structure of PCs, such as mass-spring structures and lumped mass (LM) method [20–24]. For the TM method, the analytical expression of the band gaps can be derived. However, the detailed derivation process and the expressions are simple for the 1D binary PC, and it will become very tedious for a 1D PC with multi-components and multimaterials. The disadvantage of the TM method is that it is difficult to solve the band gaps of the 2D and 3D PCs. As the continuous system is treated as discrete models in the LM method, the increment of the number of components in a unit cell cannot complicate the method futher. The method is also suitable for the 2D and 3D PCs. Compared to the PWE method, the LM method converges faster and its convergence is not affected by the difference in the elastic constants. Specifically, in the calculation of band gaps with small differences in elastic constants, the convergence of LM method is similar to that of PWE method. However, in the calculation of band gaps with large differences in the elastic constants, the LM method exhibits better convergence and higher accuracy. Although the convergence of the MST method is better than the LM method, some dispersion curves can be calculated by LM method, which is not possible by MST method. Another advantage is that the LM method does not have any restrictions regarding the shape of the unit cell of PC, which means the LM method is more widely used for PC with complicated profiles [21–24].

For the finite periodic PCs, the frequency band gap is usually calculated from frequency-response function (FRF) or transmission coefficients. The width of the band gap and the minimum FRF value of the signal inside the band gap are used to evaluate the performance of vibration isolation. The frequency band gap is usually affected by the lattice constant, the filling fraction (the fraction of one material in all) and the material parameters (density and modulus); and the value of attenuation inside the gaps will decrease quickly when the number of unit cells increases, i.e. the minimum FRF value is affected by the number of unit cells. The PC can be used in noise control, vibration shield, acoustic lens and elastic/acoustic filters. For example, it can be used in the design of acoustic diode to achieve unidirectional propagation of acoustic energy flux [24,25].

As we know, when the acoustic waves propagate through a 1D waveguide with variable cross-section, the vibration velocity of a particle and sound pressure will be changed with the cross-section. When the elastic/acoustic waves propagate through periodic structures with variable cross-sections, whether the frequency band gaps and the attenuation

performance will be changed is the question we would like to answer in this paper. After comparing the advantages and disadvantages of the methods mentioned above, the LM method is selected in this paper. We analysed a longitudinal wave propagated through a quasi-1D finite PC with conical cross-section. Unlike in the finite PC with constant section, the initial frequency, the cut-off frequency and the width of the band gap will vary with the ratio of the cross-sectional area of the input and output terminals.

2. The characteristic of longitudinal wave: The lumped mass model of the quasi-1D finite PC with conical cross-section

In the LM method, the continuous PC is divided into a finite number of particles connected by linear elastic springs. So, the finite 1D PC is simplified to many particle–spring vibrators with finite degrees of freedom, the more is the number of degrees of freedom, the closer it is to the real PC and the higher is the accuracy of the calculation [20–24]. A binary system with N unit cells which consists of alternating A and B layers is shown in figure 1a. The cells are arranged in the direction of elastic wave propagation, and due to the variable shapes, the cells are not strictly of identical repetitive units. So the structure considered in this paper is called quasi-1D PC. In the figure, a, b, l, L and n are the radii of the left (or input) terminal and right (or output) terminal, the lattice constant, the total
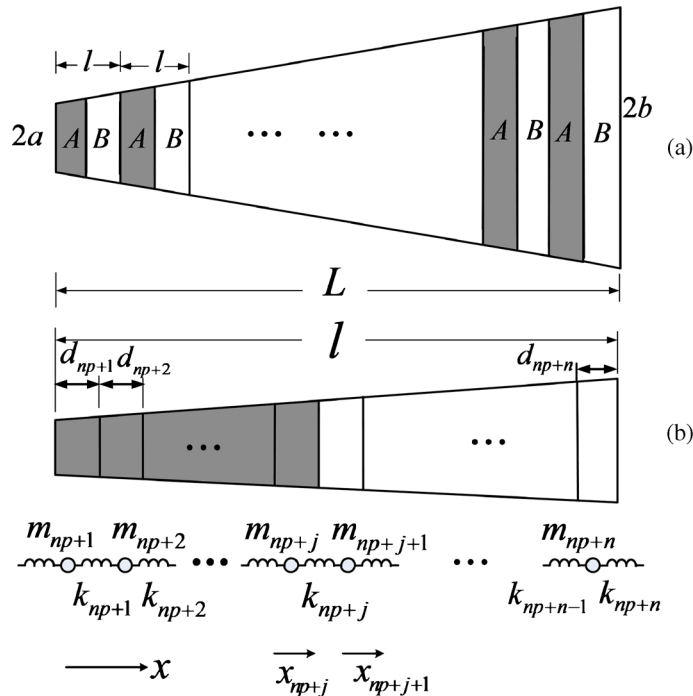

Figure 1. (**a**) A finite PC consisting of materials A and B and (**b**) a unit cell is divided into the particle–spring vibrators with n degrees of freedom ($j = 1, 2, \ldots, n$, $p = 0, 1, \ldots, N - 1$.

length of the structure and the number of particles in each cell, respectively. When a force is applied along the axial direction (x direction), a longitudinal wave will be produced. We assume that the longitudinal wave propagated in the structure is a plane-wave, and the vibration of any particle on the same plane has equal amplitude and phase, i.e. the propagation of the longitudinal wave in the structure can be simplified to a 1D problem.

Figure 1b shows a cell with n springs and particles connected in series, the stiffness is $k_{np+1} \sim k_{(p+1)n}$, the mass is $m_{np+1} \sim m_{(p+1)n}$ and the length of arbitrary adjacent simplified units is $d_{np+1} \sim d_{(p+1)n}$. Figure 2 shows a simplified unit, the point O is the gravity centre, $r_{np+j+1/2}$ is the radius at the gravity centre position, α_{np+j} is a ratio corresponding to the length d_{np+j}. In each simplified unit, there is only one material, the particle is located in the gravity centre, and on both sides of the particle, there are two springs with different stiffnesses. According to the knowledge of geometry, for every simplified unit, we have

$$r_{np+j} = a + \frac{\sum_1^{np+j-1} d_{np+j}}{L}(b-a) \quad \text{and} \quad r_1 = a, \quad r_{nN+1} = b, \tag{1}$$

$$r_{np+j+1/2} = \left(\frac{r_{np+j}^3 + r_{np+j+1}^3}{2}\right)^{1/3}, \tag{2}$$

$$\alpha_{np+j} = \frac{r_{np+j+1/2} - r_{np+j}}{r_{np+j+1} - r_{np+j}}, \quad j = 1, 2, \ldots, n, \quad p = 0, 1, \ldots, N-1. \tag{3}$$

For a simplified unit with one constant section, $\alpha_{np+j} = 1/2$.

The mass of each particle is

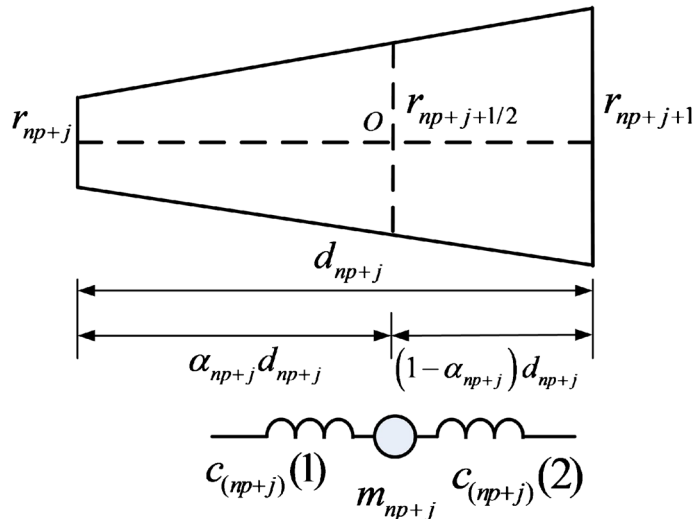$$m_{np+j} = \frac{1}{3}\pi\rho_s d_{np+j}(r_{np+j}^2 + r_{np+j+1}^2 + r_{np+j}r_{np+j+1}), \tag{4}$$

Figure 2. Geometrical diagram of a simplified unit ($j = 1, 2, \ldots, n, p = 0, 1, \ldots, N-1$.

where ρ_s (s = A, B) is the volume density. For a half simplified unit, the stress along the longitudinal direction is proportional to the strain along the same direction, and the relationships obtained are

$$\frac{F_x(1)}{S_{np+j}} = E_s \frac{\Delta x 1}{\alpha_{np+j} d_{np+j}}, \tag{5a}$$

$$\frac{F_x(2)}{S_{np+j}} = E_s \frac{\Delta x 2}{(1 - \alpha_{np+j}) d_{np+j}}, \tag{5b}$$

where E_s (s = A, B) is the Young's modulus, $F_x(1)$ and $F_x(2)$ are the applied forces on the left and right along the x direction. S_{np+j} is the cross-sectional area at the gravity centre of every simplified unit, and it is defined as $S_{np+j} = \pi r_{np+j+1/2}^2$, $\Delta x 1$ and $\Delta x 2$ are the displacement produced by the forces along the x direction for the left half simplified unit and the right half simplified unit, respectively. The compressive stiffness on both sides of the particles can be defined as follows:

$$c_{np+j}(1) = \frac{F_x(1)}{\Delta x 1} = \frac{E_s S_{np+j}}{\alpha_{np+j} d_{np+j}}, \tag{6a}$$

$$c_{np+j}(2) = \frac{F_x(2)}{\Delta x 2} = \frac{E_s S_{np+j}}{(1 - \alpha_{np+j}) d_{np+j}}. \tag{6b}$$

The springs between the adjacent particles can be considered as that in series mechanically, i.e. the spring k_{np+j} is composed of $c_{np+j}(2)$ and $c_{np+j+1}(1)$ in series. If the adjacent simplified units are made of the same materials;

$$
\begin{aligned}
k_{np+j} &= \frac{c_{np+j}(2) \cdot c_{np+j+1}(1)}{c_{np+j}(2) + c_{np+j+1}(1)} \\
&= \frac{E_s \cdot S_{np+j} \cdot S_{np+j+1}}{S_{np+j} \cdot \alpha_{np+j+1} d_{np+j+1} + S_{np+j+1}(1 - \alpha_{np+j}) d_{np+j}}, \quad s = \text{A, B},
\end{aligned}
\tag{7}
$$

if the adjacent simplified units are made of different materials, and the left material is A, the right material is B;

$$k_{np+j} = \frac{E_{\text{A}} \cdot E_{\text{B}} \cdot S_{np+j} \cdot S_{np+j+1}}{E_{\text{A}} \cdot S_{np+j} \cdot \alpha_{np+j+1} d_{np+j+1} + E_{\text{B}} \cdot S_{np+j+1}(1 - \alpha_{np+j}) d_{np+j}}, \tag{8a}$$

otherwise, the left material is B, the right material is A.

$$k_{np+j} = \frac{E_{\text{A}} \cdot E_{\text{B}} \cdot S_{np+j} \cdot S_{np+j+1}}{E_{\text{B}} \cdot S_{np+j} \cdot \alpha_{np+j+1} d_{np+j+1} + E_{\text{A}} \cdot S_{np+j+1}(1 - \alpha_{np+j}) d_{np+j}}. \tag{8b}$$

For a cell, which contains various materials, it can also be simplified to the particle–spring vibrators in an analogous method.

In this paper, the lengths of arbitrary adjacent simplified units are supposed to be equal to each other, i.e. $d = d_1 = d_2 = \cdots d_{np+j} \cdots = d_{nN}$, and $d = L/(nN)$. For $np + j$ particles, the motion equations

$$m_{np+j} \frac{d^2 x_{np+j}}{dt^2} = k_{np+j}(x_{np+j+1} - x_{np+j}) - k_{np+j-1}(x_{np+j} - x_{np+j-1}), \quad (9)$$

where x_{np+j} is the displacement. Discretizing the time t, the differential equation (9) can be transformed into different equations:

$$x_{np+j}[(i+1)\Delta t] = \frac{\Delta t^2}{m_{np+j}} \{k_{np+j}[x_{np+j+1}(i\Delta t) - x_{np+j}(i\Delta t)]$$

$$-k_{np+j-1}[x_{np+j}(i\Delta t) - x_{np+j-1}(i\Delta t)]\}$$

$$-x_{np+j}[(i-1)\Delta t] + 2x_{np+j}(i\Delta t),$$

$$np + j = 2, 3, \ldots, nN - 1, \quad (10a)$$

$$x_{nN}[(i+1)\Delta t] = -\frac{\Delta t^2}{m_{nN}} k_{nN-1}[x_{nN}(i\Delta t) - x_{nN-1}(i\Delta t)]$$

$$-x_{nN}[(i-1)\Delta t] + 2x_{nN}(i\Delta t), \quad np + j = nN, \quad (10b)$$

where i is an integer and Δt is the discrete time interval. A periodic initial displacement $A_0 \cos(\omega t)$ (where A_0 is the displacement amplitude and ω is the angular frequency) is subjected to the input terminal x_1, then the output displacement x_{nN} at every time can be obtained using eq. (10). Finally, comparing x_{nN} with the original displacement x_1, the FRF of the particle–spring structure can be obtained as FRF $= 20 \lg (x_{nN}/x_1)$.

3. Theoretical results – the effect of geometrical parameters on the band gap

As a comparison between 1D finite PC with constant section and conical section, we considered a binary periodic system of A – PMMA (polymethyl methacrylate) and B – duralumin layers. The model of the structure with N cell is shown in figure 1a, and the corresponding discrete particle–spring model of a cell is shown in figure 1b. The structure is subjected to a periodic displacement loading $A_0 \cos(\omega t)$ at the input terminal.

Figure 3 displays the FRF curves with different ratios of cross-sectional area, β of the input and output ends $(\beta = S_{out}/S_{input} = (b/a)^2)$. In the calculation, the lattice constant $l = 40$ mm, the periodic number $N = 5$, the number of particles in each cell $n = 20$, and the filling fraction $\eta = l_A/l = 0.5$, where l_A is the length of the material A in a cell; for $\beta = 9$ and $\beta = 1$, $a = 2$ mm, however, for $\beta = 0.11$, $b = 2$ mm. The material parameters employed in the calculations were $\rho_{Al} = 2790$ kg/m^3, $E_{Al} = 7.15 \times 10^{10}$ Pa, $\rho_{pmma} = 1142$ kg/m^3, $E_{pmma} = 0.2 \times 10^{10}$ Pa. In the analysis, the frequencies corresponding to FRF $= 0$ on two sides of the band gap are, respectively, defined as the initial frequency and the cut-off frequency. From figure 3, it can be seen that there are two band gaps in the frequency range 0–70 kHz for each curve. When the ratio of the cross-sectional area of the input and output terminals increases, the attenuation of the signal inside both the first band gap and second band gap will decrease quickly. For $\beta = 9$, the
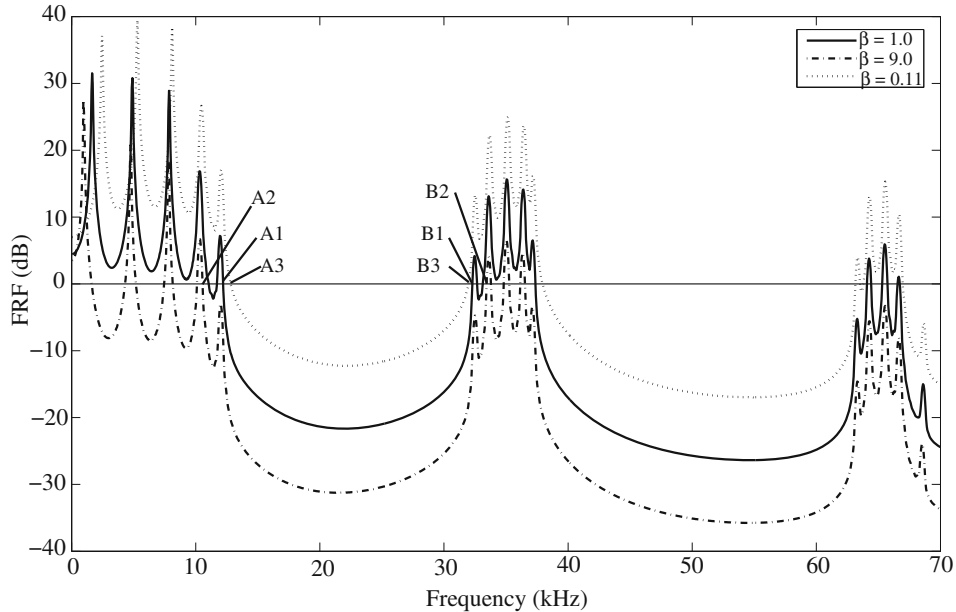
Figure 3. FRF curves for the 1D finite binary PC with ratios of different cross-sectional area, β.

attenuation of the FRF curve decreases the fastest; the initial frequency of the first band gap at point A2 is lower than at points A1 and A3, and the cut-off frequency of the first band gap at point B2 is higher than at points B1 and B3. (In the later parts of this paper, the initial frequency and the cut-off frequency also belong to the first band gap.) In the figure, the minimum FRF value of the curve $\beta = 9$ is -32 dB, and for the curve $\beta = 1$, the minimum FRF value is -22 dB, i.e. the minimum FRF value of the curve increases as β increases. As we know, when β increases, the mass of the structure also increases. So, the reduced transmission levels can be also explained as the increase in mass of the structure.

Figure 4 shows the relationship between the frequencies (initial frequency and cut-off frequency) and the ratio of cross-sectional area, β. We can see that the initial frequency decreases as the ratio β increases while the cut-off frequency increases with the ratio β. In other words, the width of the band gap increases with the ratio β. The leaps of the curves that appear in figure 4, is due to the increase in β. The FRF value of the peaks will be less than zero, and the frequencies will change suddenly. For example, in figure 3, there are two peaks inside the first band gap for the curve $\beta = 9$. From figures 3 and 4, we can see that the attenuation performance can be improved and the width of the band gap can be expanded by increasing the cross-sectional area of the output end. These properties may be helpful in the manufacture of vibration shield and elastic filters.

As we know, the PBG of a 1D PC with constant section are usually affected by the filling fraction and the lattice constant. Figure 5 displays the relationships between the frequencies (initial frequency and cut-off frequency) and the lattice constants. The solid lines represent the PC with conical section and the dotted lines represent the PC with constant section. It can be seen that the initial frequencies and the cut-off frequencies decrease as the lattice constant increases, and the width of the first band gap decreases
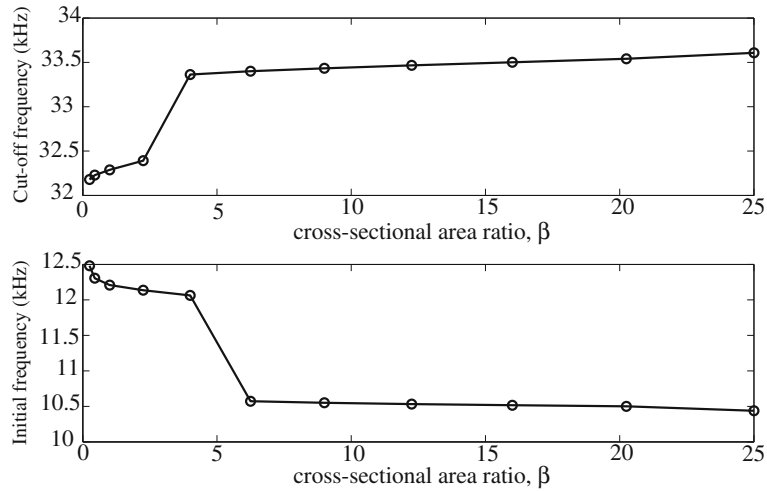
Figure 4. Relationship between the frequencies (initial frequency and cut-off frequency) and the cross-sectional area ratio, β.

as well. Figure 6 demonstrates the relationships between the frequencies and the filling fractions. We can see that the initial frequencies decrease as the filling fraction increases, and the cut-off frequencies increase first and decrease later as the filling fraction increases.
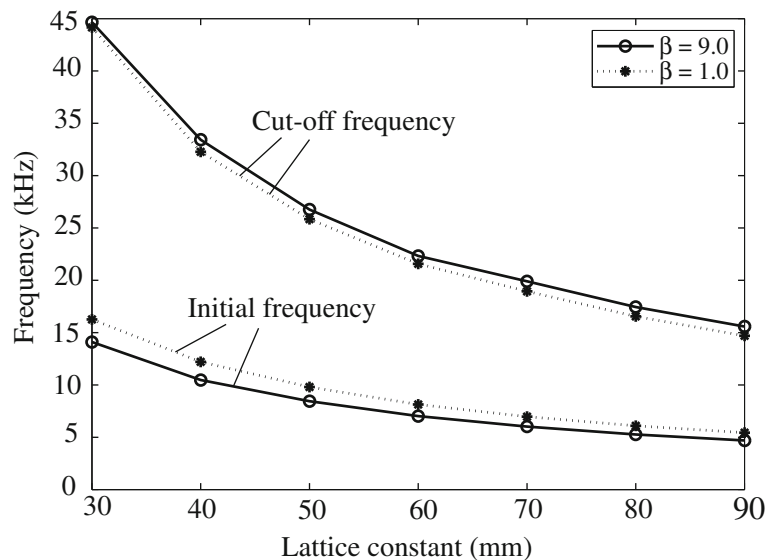

Figure 5. The relationship between the lattice constants and the frequencies. The solid lines represent the frequencies of the PC with conical section ($\beta = 9$) and the dotted lines represent those with constant section ($\beta = 1$), respectively. Here, the parameters are: $N = 5, n = 20, \eta = 0.5$ and $a = 2$ mm.
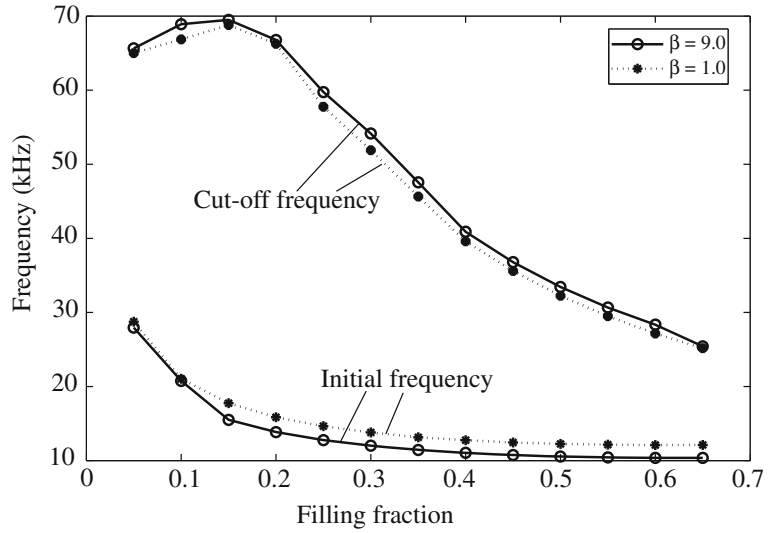
Figure 6. The relationship between the filling fractions and the frequencies. The solid lines represent the frequencies of the PC with conical section ($\beta = 9$) and the dotted lines represent those with constant section ($\beta = 1$), respectively. Here, the parameters are: $N = 5$, $n = 20$, $l = 40$ mm and $a = 2$ mm.
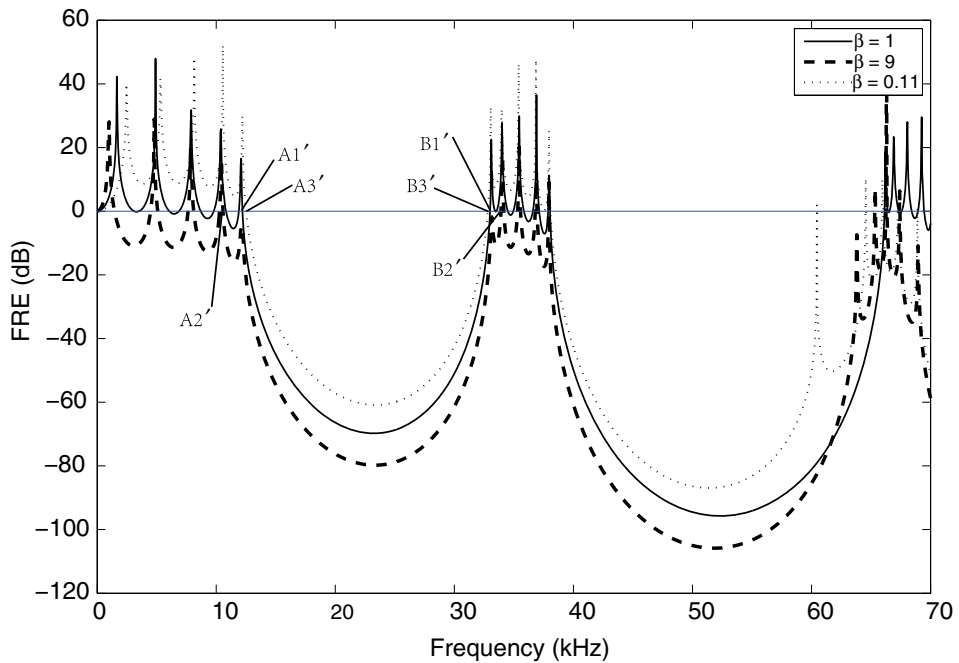

Figure 7. FRF curves simulated by the finite element software, ANSYS.

Table 1. Theoretical and simulated frequencies and minimum FRF value.

β	f_A (kHz)	f_B (kHz)	f'_A (kHz)	f'_B (kHz)	F (dB)	F' (dB)
0.11	12.81	31.97	12.51	32.81	−13	−61
1	12.21	32.28	12.21	32.98	−22	−70
9	10.55	33.43	10.57	33.91	−32	−80

When the filling fraction η is ∼0.15, the cut-off frequency and the width of the first band gap reach their maximum. In figures 5 and 6, we can see, for the finite PC with constant section, compared with the curves of conical section, that the initial frequency is higher and the cut-off frequency is slightly lower, and the width of the band gap is slightly narrower. However, the trend of change in frequencies are consistent with each other.

4. Comparison of theoretics and simulation

ANSYS is a commonly used finite element software, and its multiphysics module can be used to solve the multidisciplinary and multiphysics coupling problems, such as structure, mechanics, thermology, hydrodynamics, eletromagnetics and the coupling problem of two or more physical fields. In order to validate the theoretical analysis in this paper, those phononic crystals, which are calculated in figure 3, are simulated by the finite element software ANSYS, and the results are shown in figure 7. The initial frequencies and cut-off frequencies are listed in table 1, where f_A, f_B correspond to frequencies of points A1, A2, A3, B1, B2, B3 in figure 3; f'_A, f'_B correspond to the frequencies of points A1′, A2′, A3′, B1′, B2′, B3′ in figure 7; and F and F' are the minimum FRF values of the first band gap calculated by the method followed in this paper and the software ANSYS. When we compare, figure 7 with figure 3, the curves exhibit well-consistent change with each other. It can be seen from table 1 that the initial frequencies and cut-off frequencies using our method are in good agreement with those simulated by finite-element method. Although, differences of the minimum FRF values exist, the law that minimum FRF value increases with the area ratio β is still applicable.

5. Conclusions

In this paper, we studied the propagation of elastic longitudinal wave in quasi-1D finite PC with conical section, and derived the expressions of FRF. As we know, for finite PC, the common method to improve the attenuation performance, is to increase the number of unit cells. By analysing the FRF curves, we found that the transmission levels within the band gaps will decrease quickly, when the cross-sectional area of the output end increases. So, the attenuation performance can also be improved by increasing the cross-sectional area. At the same time, the band gaps of finite PC with conical section are wider than those with constant section. The effects of the lattice constant and filling fraction on the width of the band gap were also investigated, and the results showed that the change in the initial and cut-off frequencies are consistent with those of the constant section. Finally, the FRF curves of the finite PCs with conical section were also simulated by the finite

element software, ANSYS. It was shown that the results using this method are in good agreement with those analysed by finite element method. The method used in this paper is also appropriate to the finite PC with other variable cross-sections. We hope that this study will help in practical applications of PC.

Acknowledgement

References

[1] E Yablonovitch, *Phys. Rev. Lett.* **58**, 2059 (1987)
[2] S John, *Phys. Rev. Lett.* **58**, 2486 (1987)
[3] M M Sigalas and E N Economou, *J. Sound Vib.* **158**, 377 (1992)
[4] M S Kushwaha, *Int. J. Mod. Phys. B* **10**, 977 (1996)
[5] M S Kushwaha, P Halevi, L Dobrzynski and B Djafari-Rouhani, *Phys. Rev. Lett.* **71**, 2022 (1993)
[6] Z Liu, X Zhang, Y Mao, Y Y Zhu, Z Yang, C T Chan and P Sheng, *Science* **289**, 1734 (2000)
[7] A Diez, G Kakarantzas, T A Birks and P St J Russel, *Appl. Phys. Lett.* **76**, 3481 (2000)
[8] M Sigalas and E N Economou, *Solid State Commun.* **86**, 141 (1993)
[9] S Mizuno and S Tamura, *Phys. Rev. B* **45**, 734 (1992)
[10] M M Sigalas and C M Soukoulis, *Phys. Rev. B* **51**, 2780 (1995)
[11] S Chen, S Lin and Z Wang, *Solid State Commun.* **150**, 285 (2010)
[12] S Chen, S Lin and Z Wang, *Solid State Commun.* **148**, 428 (2008)
[13] M S Kushwaha *et al*, *Phys. Rev. B* **49**, 2313 (1994)
[14] M S Kushwaha and B Djafari-Rouhani, *J. Appl. Phys.* **88**, 2877 (2000)
[15] M M Sigalas and N García, *Appl. Phys. Lett.* **76**, 2307 (2000)
[16] S Chen, *Acta Acust. United Acust.* **94**, 388 (2008)
[17] M Kafesaki, *Phys. Rev. B* **60**, 11993 (1999)
[18] Z Liu, C T Chan and P Sheng, *Phys. Rev. B* **62**, 2442 (2000)
[19] H Karagülle, L Malgaca and H F Öktem, *Smart Mater. Struct.* **13**, 661 (2004)
[20] J S Jensen, *J Sound Vib.* **266**, 1053 (2003)
[21] J H Wen, G Wang, Y Z Liu and D L Yu, *Acta Phys. Sin.* **53**, 3384 (2004)
[22] G Wang, J Wen, Y Liu and X Wen, *Phys. Rev. B* **69**, 184302 (2004)
[23] G Wang, J Wen and X Wen, *Phys. Rev. B* **71**, 104302 (2005)
[24] G Wang, X Wen, J Wen, L Shao and Y Liu, *Phys. Rev. Lett.* **93**, 154302 (2004)
[25] B Liang, B Yuan and J C Cheng, *Phys. Rev. Lett.* **103**, 104301 (2009)
[26] B Liang, X S Guo, J Tu, D Zhang and J C Cheng, *Nature Mater.* **9**, 989 (2010)